

Influence of fault-tolerant stator structure on performance of permanent magnet bearingless slice machines

Qiang DING^{a,b}, Guyu WU^a, Zhiqian DENG^a, Xiaolin WANG^a

^aNanjing University of Aeronautics and Astronautics, Yudao street 29, 20016 Nanjing, China, dzq@nuaa.edu.cn

^bNanjing Institute of Industry Technology, North Yangshan road 1, 210023 Nanjing, China

Abstract—Fault-tolerant capability is a vital requirement for bearingless slice machine which is used in safety critical application field. This paper compares two bearingless slice machines, conventional permanent magnet bearingless slice machine and fault-tolerant permanent magnet bearingless slice machine, from fault-tolerant capability, suspension and drive performance points of view. Due to introduction of fault-tolerant stator structure, a optimization method for reduction of total harmonic distortion(THD) of back-EMF and electromagnetic coupling between different phases is proposed. Then, some relevant performance comparison, such as fault-tolerant performance, suspension performance as well as drive torque performance, is analyzed by finite element analysis. Finally, several design considerations are presented as guideline for design of bearingless slice machines with fault-tolerant stator structure.

Keywords—Machine design, permanent-magnet bearingless slice machine(PMBSM), fault-tolerant PMBSM, structure optimization

I. INTRODUCTION

During the last few years, a magnetic suspension machine technique has been successfully used in various industry field, especially for some safety critical applications, such as hazardous chemical material process, blood pumps for artificial heart assistance device and ultra-pure fluid pumps in semiconductor industry [1-2]. A bearingless machine combines a electric machine function and a magnetic bearing function [3-6]. Due to absence of mechanical bearing, it offers the advantages of no friction, no wear, lubricant- and maintenance-free operation and much longer service interval [7-8].

Stable suspension of five degrees of freedom must be achieved for conventional bearingless machine, which results in complex control system and increase of hardware cost. Thus, it blocks the development of bearingless technique in the application of limited space. In order to simplify control system and minimize hardware cost, a bearingless slice machine, which features a disk-shaped rotor, have been developed [9]. Only two radial degrees of freedom are needed active control, while one axial degree of freedom and two tilting degrees of freedom are passively stabilized by means of reluctance force.

Under safety critical application field of bearingless slice machine, two fundamental requirements, i.e., system durability and reliability, need to be considered. Due to magnetic suspension, the structure durability of machine can be enhanced drastically because bearing failure accounts for high possibility of machine failure. As for the

control system reliability, only two radial positions need to be actively controlled because of disk-shaped rotor design. Thus, the number of power electronic devices and computational burden of digital signal processor are decreased. Certainly, the control system reliability is enhanced from control point of view. However, the system reliability also depends on the machine structure. Once it appears failure during operation, the machine must have capability (so-called fault-tolerant capability) to prevent further development of the failure. Meanwhile, it must have little impact on healthy components and exists sufficient healthy phase windings to keep stable operation for a period of time. Thus, the system reliability can not be enhanced if no specific fault-tolerant design is performed. However, to the best knowledge of the authors, there is a little available literature about fault-tolerant design of bearingless slice machine. In the preceding study of our research team in [7], the authors studied the fault-tolerant controllability of bearingless slice motor and gave theoretical analysis with emphasis on control strategy. However, the motor topology in [7] has no fault-tolerant capability. In [8-13], several topologies of bearingless slice motor were proposed and one of them, which has E-shape stator structure, has possibility of fault-tolerant operation. Nevertheless, the fault-tolerant operation can not be achieved because it is a two-phase motor. There are insufficient phase windings to keep operation when appearing failure in windings. In [14-16], a series of bearingless slice segment motors with four-, five- and six stator elements and surface mounted rotor magnets were proposed. In [17], a bearingless slice segment motor with four stator elements and halbach magnet ring rotor was designed. In [18], a bearingless slice segment motor with four stator elements and consequent pole rotor was delivered. In [19], a bearingless slice segment motor with five stator elements and axial magnetized rotor magnets was achieved. All these bearingless slice segment motors features no mutual inductance between different phases and the number of stator elements is larger than three, thus, this type of bearingless slice motor possesses potential fault-tolerant capability. However, due to stator segment it is difficult obtain analytical model between control currents and suspension force as well as torque, that is to say, some key parameters must be calculated by 2D or 3D finite element simulation for closed-loop control. Thus, the control algorithm loses its generality.

In this paper, a fault-tolerant stator structure is utilized for PMBSM to increase fault-tolerant capability and its influence on the machine performance is also studied and analyzed. Except for the stator structure, the rotor structure,

main dimensions and machine materials of the fault-tolerant PMBSM in this paper are the same as our preceding work in [7], the aim of which is to keep the comparison as fair as possible. The fault-tolerant PMBSM consists of six-phase combined concentrated windings, which generates drive torque and bearing force simultaneously. The optimized stator shape with unequal tooth width between armature teeth and fault-tolerant teeth is for increase of fault-tolerant capacity. However, when the pole-pair number of rotor is one, the introduction of fault-tolerant teeth result in distortion of no-load back-EMF. Thus, a optimization method is proposed for reduction of total harmonic distortion of no-load back-EMF, which is helpful for decreasing torque ripple and increasing control performance. The detailed optimization process will be presented. Finally, drive and levitation performance comparison of fault-tolerant PMBSM and PMBSM is performed to show the influence of the fault-tolerant stator structure.

II. STRUCTURE AND ADVANTAGES

The fault-tolerant PMBSM proposed in this paper is depicted in Fig.1. There are twelve stator teeth with unequal tooth width, where the narrow teeth are fault-tolerant tooth and the wide teeth are armature tooth. Because the fault-tolerant teeth have little contribution to suspension force and torque, smaller tooth width than armature teeth is beneficial to increase slot area. It can be seen from Fig.1 that the shape of armature teeth is similar to duck flipper and the distances from inner edge of armature teeth and fault-tolerant teeth to centre point are different. All these design considerations are to reduce harmonic content of back-EMF.

If the fault-tolerant PMBSM is driven by six H-bridge inverters, it leads to three advantages from fault tolerance point of view. To begin with, it could achieve thermal isolation under short circuit condition because adjacent phase windings are in different stator slot. In addition, the it features magnetic isolation capability due to existence of fault-tolerant teeth and adoption of single-layer non-overlapping concentrated windings. That is to say, the healthy phases are difficult to be infect with the faulty phases. Third, the utilization of H-bridge inverter results in the electrical isolation between different phases.

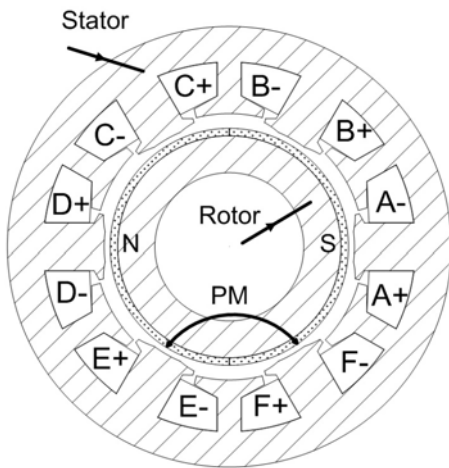


Figure 1. Structure of fault-tolerant PMBSM

III. OPTIMIZATION DESIGN AND PERFORMANCE ANALYSIS

A. Stator Structure optimization

To reduce mutual inductance of inter-phase is a key issue with respect to the magnetic isolation. It can be achieved by introduction of fault tooth between adjacent armature teeth. However, the back-EMF deviates from sinusoidal waveform compared with its original stator structure. Thus, the maximum ratio of mutual inductance over self inductance (signed as $\max(M/L)$) and the total harmonic distortion of back-EMF (signed as THD) are two variables needed to be considered and the target values of them are set as $\max(M/L) \leq 5\%$ and $\text{THD} \leq 3\%$.

In order to achieve optimization design, three structure variables of stator, W_f , L_g and θ shown in Fig.2, which are defined as width of fault-tolerant tooth, difference between fault-tolerant tooth radius and armature tooth radius, slot opening angle between two adjacent armature teeth respectively, are investigated by FEM. The results of this investigation provide the guideline for fault-tolerant PMBSM design.

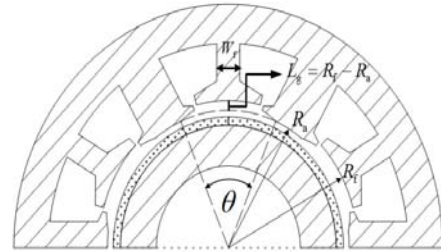


Figure 2. Definition of structure parameters for optimization

The detailed optimization process is as follows:

1. To adjust W_f and remain L_g , θ unchanged

$$\begin{cases} \text{THD}_{E_0} = f_1(W_f, L_g, \theta) | \theta = \text{const}, L_g = \text{const} \\ \max(M/L) = \tau_1(W_f, L_g, \theta) | \theta = \text{const}, L_g = \text{const} \end{cases} \quad (1)$$

where M and L are values of mutual inductance and self-inductance respectively.

It can be observed in Fig.3 that to change W_f has insignificant variations with respect to $\max(M/L)$ and THD when W_f is smaller than eight millimeters. Hence, what should be considered to determine W_f is its influence on the slot area.

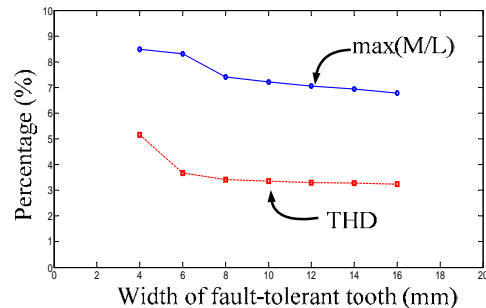


Figure 3. Influence of the fault-tolerant width on the $\max(M/L)$ and THD of back-EMF

2. To adjust L_g and remain W_f, θ unchanged

$$\begin{cases} THD_{E_0} = f_2(L_g, W_f, \theta) | W_f = const, \theta = const \\ \max(M/L) = \tau_2(L_g, W_f, \theta) | W_f = const, \theta = const \end{cases} \quad (2)$$

In this step, five samples of L_g , which is adjusted from 1mm to 5mm, are taken into account. Fig.4 shows the variation tendency of $\max(M/L)$ and THD. It can be observed that the variation tendency of THD is to decrease while $\max(M/L)$ is to increase with respect to the variation of L_g . Thus, there is a trade-off when to determine L_g .

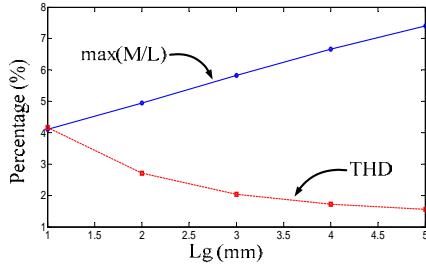


Figure 4. Influence of the eccentric distance of fault-tolerant tooth on the $\max(M/L)$ and THD of back-EMF

3. To adjust θ and remain W_f, L_g unchanged

$$\begin{cases} THD_{E_0} = f_3(\theta, L_g, W_f) | L_g = const, W_f = const \\ \max(M/L) = \tau_3(\theta, L_g, W_f) | L_g = const, W_f = const \end{cases} \quad (3)$$

It can be observed in Fig.5 that the variation tendency of $\max(M/L)$ and THD is to decrease simultaneously when the variable θ is to increase. Hence, to adjust θ is an effective method to achieve optimization objectives. However, it can be seen from Fig.6 that there is a trade-off because the adjustment of θ lead to the decrease of root-mean-square value of back-EMF.

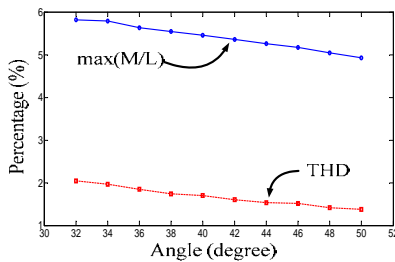


Figure 5. Influence of the angle θ on the $\max(M/L)$ and THD of back-EMF

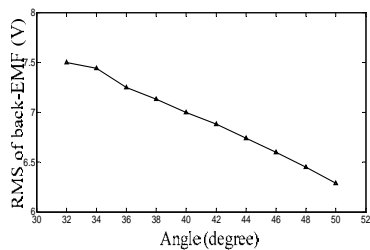


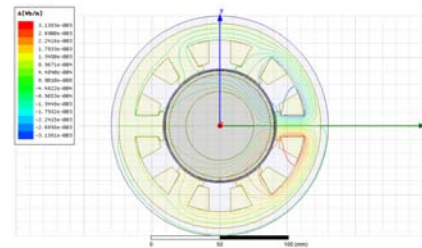
Figure 6. Influence of the angle θ on RMS value of back-EMF

B. Fault-tolerant capability analysis

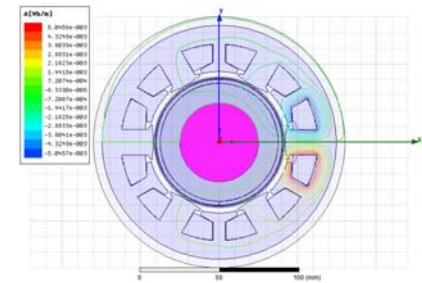
Based on above-mentioned three optimization steps, the specifications of fault-tolerant PMBSM are listed in Table I. In order to show comparison between before and after optimization, the specifications of PMBSM in [7] are also listed.

Items	Bearingless Machine
Stator outside diameter	149mm
Stator inner diameter	84mm
Rotor inner diameter	50mm
Axial length	10mm
Number of stator slots	6 (PMBSM)
	12 (fault-tolerant PMBSM)
Number of PMs	2
Air gap length	2mm (PMBSM)
	2mm to 5mm (fault-tolerant PMBSM)
Width of armature tooth	16mm
W_f	8mm(fault-tolerant PMBSM)
L_g	3mm(fault-tolerant PMBSM)
θ	46 degree(fault-tolerant PMBSM)

Fig.7 shows the flux distribution of the two machines, in which only phase-A is excited and the magnets are unmagnetized for clarity. It can be observed that the large quantity of flux lines pass through the fault-tolerant tooth and small quantity of flux lines couple with other phases in fault-tolerant PMBSM, whereas the number of flux lines which couple with the other phases in PMBSM are larger than the number in fault-tolerant PMBSM. This means that fault-tolerant PMBSM has weak coupling between phases, whereas PMBSM has strong coupling between phases. The significant inter-phase coupling indicates that once a fault occurs in one phase, it would have an undesirable impact on other healthy phases.



(a) PMBSM



(b) Fault-tolerant PMBSM

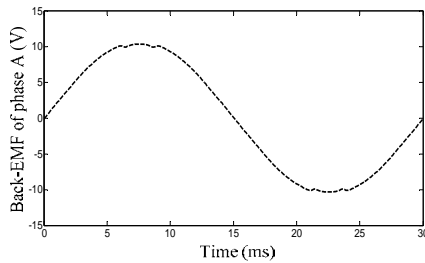
Figure 7. Flux distribution of PMBSM and fault-tolerant PMBSM

Table II compares self- and mutual inductance of phase-A between PMBSM and fault-tolerant PMBSM. The max(M/L) values of PMBSM and fault-tolerant PMBSM are 17.71% and 4.96% respectively, which demonstrates that electromagnetic coupling in PMBSM is much more serious than that in fault-tolerant PMBSM and its value of fault-tolerant PMBSM satisfies the target value($\leq 5\%$). Furthermore, the self-inductance in fault-tolerant PMBSM is larger than that in PMBSM, it means that fault-tolerant PMBSM possesses the better short-circuit current restraint capability than PMBSM under winding short-circuit failure condition.

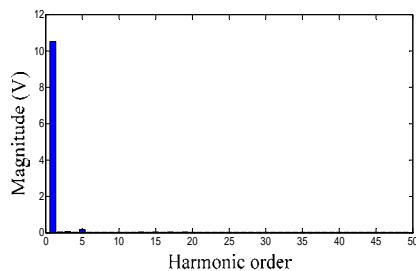
Table II Self- and mutual inductance in phase-A

	PMBSM		fault-tolerant PMBSM	
	Inductance(mH)	Percentage	Inductance(mH)	Percentage
L(A,A)	15.70	100%	25.20	100%
M(A,B)	2.78	17.71%	1.25	4.96%
M(A,C)	2.46	15.67%	1.16	4.60%
M(A,D)	2.42	15.41%	1.14	4.52%
M(A,E)	2.46	15.67%	1.16	4.60%
M(A,F)	2.78	17.71%	1.25	4.96%

Fig.8(a) illustrates the back-EMF waveform of phase A in fault-tolerant PMBSM at 2000rpm. Fig.8(b) shows its harmonic analysis. The THD value of phase A back-EMF equals to 1.51%. Thus, the high sinusoid degree of back-EMF can be achieved and satisfy its target value($\leq 3\%$) based on the optimization method above mentioned.



(a) Back-EMF of Phase A



(b) Harmonics analysis of back-EMF in phase-A

Figure 8. Waveforms of back-EMF and its harmonics analysis

C. Suspension and drive performance analysis

In this section, the suspension force and drive torque performance of PMBSM and fault-tolerant PMBSM will be compared.

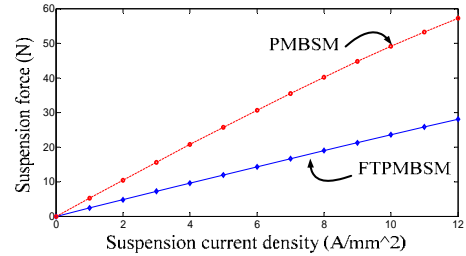


Figure 9. Comparison of suspension force

Fig. 9 demonstrates that suspension force generation capability at different suspension current density. It can be calculated from Fig.9 that the suspension force per unit levitation current density are 4.77N and 2.34N in PMBSM and fault-tolerant PMBSM respectively. Thus, there is 51% loss of suspension force in fault-tolerant BSM compared with PMBSM.

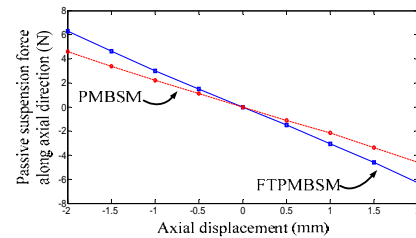


Figure 10. Comparison of passive suspension force in axial direction

Fig. 10 shows that passive levitation capability in axial direction when the rotor is in the centre of stator bore. It can be calculated from Fig.10 that the axial passive suspension force per unit axial displacement are -3.15N and -2.30N in PMBSM and fault-tolerant PMBSM respectively. Thus, there is 27% loss of axial passive levitation force in fault-tolerant PMBSM compared with PMBSM.

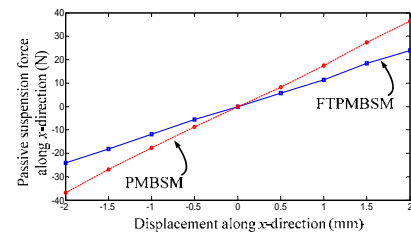


Figure 11. Comparison of passive suspension force in x direction

Fig. 11 shows that passive levitation capability in x-direction when the rotor at 0 degree position which is the rotor position shown in Fig.1. It can be calculated from Fig.11 that the passive suspension force per unit displacement are 11.98N and 18.33N in PMBSM and fault-tolerant PMBSM respectively. Thus, there is 35% reduction of horizontal passive suspension force in fault-tolerant PMBSM compared with PMBSM.

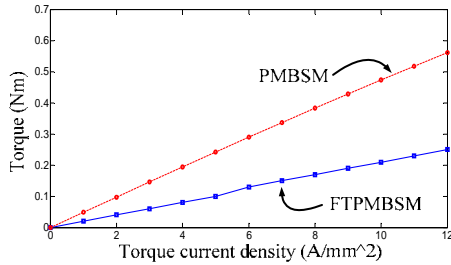


Figure 12. Comparison of torque

Fig. 12 demonstrates that torque generation capability at different torque current density. It can be calculated from Fig.12 that the torque per unit torque current density are 0.047Nm and 0.021Nm in PMBSM and fault-tolerant PMBSM respectively. Thus, there is 55% loss of torque generation capability in fault-tolerant PMBSM compared with PMBSM.

D. Design considerations

In this paper, performance comparison of two bearingless slice machines, PMBSM and fault-tolerant PMBSM, are investigated with respect to their fault-tolerant capability, suspension and drive performance. Based on performance comparison, there are some design considerations needed to be presented.

Firstly, the fault-tolerant stator structure and its optimization method can enhance fault-tolerant capability of this machine.

However, secondly, due to introduction of fault-tolerant stator structure and its optimization method, the active suspension force and drive torque performance decrease drastically. That is to say, enhancement of fault-tolerant capability is at the expense of loss of active suspension force and drive torque. There are two reasons for this result: one is the reduction of effective stator slot area due to the existence of fault-tolerant teeth; another is the increase of effective air gap length due to the optimization method.

Thirdly, for increase of active suspension force and drive torque performance, the following measures can be used based on the optimization process. The first is to decrease of main mechanical air gap length, which is defined as the difference between armature tooth inner radius and rotor radius. The second is to reduce parameter L_g , however, it should consider the increase of THD of back-EMF. The third is to decrease parameter θ , but it will lead to increase electromagnetic coupling between inter-phase.

IV. CONCLUSION

Bearingless slice machines with and without fault-tolerant stator are investigated in this paper. Three stator structure variables are defined for the stator shape optimization in fault-tolerant PMBSM. According to the proposed three optimization steps, the maximum ratio of mutual inductance over self inductance and the total harmonic distortion of back-EMF can be optimized and satisfied the target values. Then, the performance, such as fault-tolerant capability, suspension force and drive torque

generation, of PMBSM and fault-tolerant PMBSM are compared and analyzed. The results of comparison and analysis show that fault-tolerant PMBSM have better fault-tolerant capability than PMBSM, nevertheless its suspension and drive performance is weaker than PMBSM due to small stator area and large air gap length. Thus, three design considerations are presented for fault-tolerant PMBSM to enhance suspension and drive performance.

REFERENCES

- [1] M. Neff, N. Barletta, and R. Schöb, "Magnetically levitated centrifugal pump for highly pure and aggressive chemicals," in Proc. PCIM Conf., Nuremberg, Germany, Jun. 6–8, 2000.
- [2] N. Barletta and R. Schöb, "Design of a bearingless blood pump," in Proc. 3rd Int. Symp. Magn. Suspension Technol., Tallahassee, FL, 1995, pp. 265–274.
- [3] F. Zürcher, T. Nussbaumer, and J.W. Kolar, "Motor torque and magnetic levitation force generation in bearingless brushless multipole motors," IEEE/ASME Trans. Mechatron., vol. 17, no. 6, pp. 1088–1097, Dec. 2012.
- [4] J. Asama, R. Kawata, T. Tamura, T. Oiwa, and A. Chiba, "Reduction of force interference and performance improvement of a consequent-pole bearingless motor," Precis. Eng., vol. 36, no. 1, pp. 10–18, Jan. 2012.
- [5] T. Reichert, T. Nussbaumer, and J. W. Kolar, "Bearingless 300-W PMSM for bioreactor mixing," IEEE Trans. Ind. Electron., vol. 59, no.3, pp. 1376–1388, Mar. 2012.
- [6] W. Gruber, T. Nussbaumer, H. Grabner, and W. Amrhein, "Wide air gap and large-scale bearingless segment motor with six stator elements," IEEE Trans. Magn., vol. 46, no. 6, pp. 2438–2441, Jun. 2010.
- [7] X.L.Wang, Q.C. Zhong, Z.Q. Deng, S.Z. Yue, "Current-Controlled Multiphase Slice Permanent Magnetic Bearingless Motors With Open-Circuited Phases: Fault-Tolerant Controllability and Its Verification," IEEE Trans. Ind. Electron., vol.59, no.5, pp. 2059–2072, May, 2012.
- [8] M.T.Bartholet, T.Nussbaumer, S. Silber, J.W. Kolar, "Comparative Evaluation of Polyphase Bearingless Slice Motors for Fluid-Handling Applications," IEEE Trans. Ind. Appl., vol.45, no.5, pp. 1821–1830, Sep. 2009.
- [9] R. Schoeb and N. Barletta, "Principle and application of a bearingless slice motor," JSME Int. J. Ser. C, vol.40, pp.593–598, 1997.
- [10] M. T. Bartholet, T. Nussbaumer, D. Krahenbuhl, F. Zurcher, and J. W. Kolar, "Modulation concepts for the control of a two-phase bearingless slice motor utilizing three-phase power modules," IEEE Trans. Ind. Appl., vol. 46, no. 2, pp. 831–840, Mar. 2010.
- [11] M. T. Bartholet, T. Nussbaumer, and J.W. Kolar, "Comparison of voltage source inverter topologies for two-phase bearingless slice motors," IEEE Trans. Ind. Electron., vol. 58, no. 5, pp. 1921–1925, May 2011.
- [12] S. Silber, W. Amrhein, P. Bösch, R. Schöb, N. Barletta, "Design aspects of bearingless slice motors," IEEE Trans. Mecha., vol.10, no.6, pp. 611–617, Dec. 2005.
- [13] K. Raggl, T. Nussbaumer, and J.W. Kolar, "A comparison of separated and combined winding concepts for bearingless centrifugal pumps," Journal of Power Electronics, Vol.9, no.2, pp. 243–258, Mar. 2009.
- [14] W. Gruber, W. Amrhein, "Design of a bearingless motor," Proc. 10th Int. Sym. Magnetic Bearing, pp. 252–257, Aug. 2006
- [15] W. Gruber, W. Amrhein, M. Haslmayr, "Bearingless segment motor with five stator elements—design and optimization," IEEE Trans. Ind. Appl., Vol.45, no.4, pp. 1301–1308, Jan. 2009.
- [16] W. Gruber, T. Nussbaumer, H. Grabner and W. Amrhein, "Wide air gap and large-scale bearingless motor with six stator elements," IEEE Trans. Magnetics, Vol.46, no.6, pp. 2438–2441, Jun. 2010.
- [17] G. Bramerdorfer, G. Jungmayr, W. Amrhein, W. Gruber, E. Marth and M. Reisinger, "Bearingless segment motor with halbach magnet," Proc. Int. Sym. Power Electronics, Electrical Drives, Automation and Motion, pp.1466–1471, 2010.

- [18] T. Stallinger, W. Gruber, W. Amrhein, "Bearingless segment motor with a consequent pole rotor," IEEE Int. Electrical Machines and Drives Conference, pp. 1374-1380, May 2009.
- [19] W. Gruber, J. Passenbrunner, G. Bramerdorfer and W. Amrhein, "Novel bearingless segment motor design with axial magnetized rotor magnets," Proc. 8th Int. Power Electronics-ECCE Asia, pp. 2225-2232, May, 2011